NANOSYSTEMS:
PHYSICS, CHEMISTRY, MATHEMATICS

Original article

Larionov K.S., et al. *Nanosystems: Phys. Chem. Math.*, 2023, **14** (6), 652–659.
http://nanojournal.ifmo.ru
DOI 10.17586/2220-8054-2023-14-6-652-659

Slow zinc release from carboxymethylcellulose gels filled with humic zinc oxide nanocomposites

Konstantin S. Larionov[1,a], Alexander Volikov[1,b], Nikita A. Sobolev[1,c], Daniil A. Kozlov[2,d], Irina V. Perminova[1,e]

[1]Lomonosov Moscow State University, 119991 Moscow, Russia

[2]Kurnakov Institute of General and Inorganic Chemistry of RAS, 119991 Moscow, Russia

[a]konstantin.larionov@chemistry.msu.ru, [b]ab.volikov@gmail.com, [c]n.a.sobolev@outlook.com, [d]kozlov@inorg.chem.msu.ru, [e]iperm@med.chem.msu.ru

Corresponding author: Irina V. Perminova, iperm@med.chem.msu.ru

ABSTRACT The study is focused on characterization of humic zinc oxide nanocomposites and their potential application in wound healing as antibacterial agent. Zinc oxide nanoparticles were synthesized with varying concentrations of humic substances (HS) and analyzed using PXRD, TEM, SEM and UV-Vis techniques. The nanoparticle sizes based on the PXRD data decreased ranged from 50 to 15 nm along with an increase in humic ligand concentration. TEM images revealed that the star-shaped aggregates of 200–500 nm ZnO particles were formed in the absence of HS, whereas the presence of humic ligands led to shapeless smaller particles ranging from 20 to 200 nm. UV-Vis spectra showed increasing of zinc oxide band gap caused with an rise of HS concentration. The band gap of ZnO nanoparticles increased from 3.19 eV to 3.40 eV as the concentration of HS increased up to 15 g/L. The synthesized ZnO-HS nanocomposites were used for filling in the hydrogels of carboxymethylcellulose (CMC). The release studies of zinc ions from the gel into different buffers were conducted to imitate wound conditions. The measurements of Zn concentrations over time in buffer showed a gradual release over time making these gels potentially suitable for long-term wound treatment.

KEYWORDS humic substances, zinc oxide nanoparticles, release, wound healing.

ACKNOWLEDGEMENTS This work was funded by the Russian Science Foundation (grant #20-63-47070). The research was carried out using the equipment of MSU Shared Research Equipment Centre "Technologies for obtaining new nanostructured materials and their complex study", "Nanochemistry and Nanomaterials" and purchased by MSU in the frame of the Equipment Renovation Program (National Project "Science and Universities") and in the frame of the MSU Program of Development.

FOR CITATION Larionov K.S., Volikov A., Sobolev N.A., Kozlov D.A., Perminova I.V. Slow zinc release from carboxymethylcellulose gels filled with humic zinc oxide nanocomposites. *Nanosystems: Phys. Chem. Math.*, 2023, **14** (6), 652–659.

1. Introduction

Development of novel biologically active and reactive nanomaterials is a dynamic field of research that has emerged in recent decades due to the intensive development of nanotechnology. Nanoparticles (NPs) have attracted considerable attention in both biomedicine and environmental remediation because of their high reactivity connected to high area-to-volume ratio and the presence of a large number of active sites. Recent reviews on the use of engineered nanomaterials as antimicrobial agents and for wound healing show the great potential of nanoparticles for biomedical applications [1–3]. Among synthetic nanoparticles, zinc oxide nanoparticles are of substantial importance [4]. A use of zinc oxide NPs as a source of slow-release zinc was shown to accelerate healing of chronic wounds [1, 5, 6]. There are many mechanisms of antimicrobial activity of zinc oxide nanoparticles including binding to thiol groups of bacterial proteins, participation in generation of reactive oxygen species (ROS), and physical interaction with bacteria [7]. Zinc oxide NPs are produced by a variety of methods [8] including thermal evaporation [9], hydrothermal synthesis [10], sol-gel technique [11], microwave synthesis [12], wet chemical precipitation [2], etc. Still, the most common method includes wet chemical precipitation because it is cheap, simple and allow to obtain high yields of NP [2]. This technique implies precipitation of $Zn(OH)_2$ from a solution of Zn^{2+} precursor (sulphate, chloride, acetate) by interaction with an alkali followed by decomposition into ZnO NPs [8].

Along with beneficial reactive properties, the use of NPs in biomedicine is of great public concern due to nanotoxicity [13]. Due to their size they can penetrate through cellular barriers. To solve this problem, the NPs are packed into "nanocontainers" made of polymeric materials by modifying the surface of NPs. For this purpose, NPs are prepared in

the presence of surfactants or ligand exchange is applied on the surface of synthesised NPs [14]. Polyethyleneglycol, polyethylene-vinylacetate, polyvinylpyrrolidone, polylactate-glycolic acid, and polyvinyl alcohol are often used as polymer compounds [15]. Among natural polymers, chitosan occupies the leading position [16], followed by collagen [17], gelatin [18], and hyaluronic acid [19]. They are usually used to stabilise NPs in aqueous media, which are most widely used in biomedical technologies. The advantage of packing NPs in nanocontainers is a significant decrease in cytotoxicity of nanoparticles with passivated surface compared to nonstabilised NPs [15]. Another promising class of natural polyelectrolytes is humic substances (HS), which are present in all natural environments and can be obtained on an industrial scale from oxidised lignite, peat, and other natural resources. Šebesta et al., 2019 [20] showed the positive effect of HS ligands in sol-gel synthesis of ZnO NPs. However, the authors conducted synthesis at one concentration of HS, whereas systematic studies at different conditions are essential.

HS are natural polyelectrolytes dominated with carboxyl and hydroxyl groups [21]. Polyfunctional character determines a wide range of their chemical interactions. They can be oxidized by strong oxidizing agents, act as reducing agents, participate in protolytic, ion exchange, and complexation reactions, participate in donor-acceptor interactions, form hydrogen bonds, and participate in van der Waals interactions [22]. The unique combination of these properties indicates high potential of HS use for biomedical and environmental applications [23–25]. A lot of publications are dedicated to a use of HS for modification of NPs [26, 27]. They can act as stabilizing agents preventing aggregation of magnetic iron oxide nanoparticles in aqueous solutions [28], they inhibit growth and crystallinity of iron oxide NPs [29, 30]. The advantage of using HS over synthetic polymers is its biocompatibility, which reduces the risk of harm to living organisms due to the release of nanoparticles [31], as well as the immunostimulatory properties of HS [32].

Another concern with the use of zinc nanoparticles is how they are applied to wounds. Usually, gels or ointments are used, which are easy to apply because of their viscosity, and the nanoparticles are also consumed evenly, which is also an advantage. Many of the biomaterials used in the synthesis of ZnO nanoparticles are also good matrices due to their gel-forming properties, such as alginate [33], chitosan [16], gelatin [34], and sago starch [35]. There is also an approach in which synthesized zinc oxide nanoparticles are placed in a gel after synthesis, for example, using amphiphilic polymers such as Carbopol [36] or N,N-dimethylacrylamide (DMAA) [37]. Carboxymethylcellulose (CMC) has also found wide application, both as a direct agent in the synthesis of zinc oxide nanoparticles [38, 39] and as a separate matrix [40]. The advantage of CMC is its availability, low cost, and nontoxicity, which allows it to be widely used in the medical and food industries.

Thus, the production of nanocompositions based on zinc nanoparticles is an urgent task. The use of humic substances will expand the possibilities of zinc oxide nanoparticles. In view of the lack of humic substances of gel-forming properties, in this work a CMC was used as one of the most convenient gel matrices.

2. Materials and methods

2.1. Materials

Commercial potassium humate (Powhumus, Humintech GmbH, Germany) isolated from leonardite has been used as a humic material (CHP). Sodium carboxymethylcellulose (CMC) with a substitution of 1.03 degrees (FL9, Wuxi, China) was used to create gels. All water solutions were prepared using the Simplicity 185 system using deionised water (Millipore, Merck KGaA, Darmstadt, Germany). The pH of the solution was measured with the Ecotest-2000 pH meter (Econix, Moscow, Russia), equipped with a universal glass electrode. Analytical grade reagents ($Zn(OAc)_2$, NaOH) were used to synthesise zinc oxide nanoparticles and adjust pH.

2.2. Synthesis of humic zinc oxide nanocomposites

ZnO-NPs were synthesized by the method of alkaline precipitation in aqueous solution of HS using an approach described by [20]. The experimental setup is shown in Fig. 1.

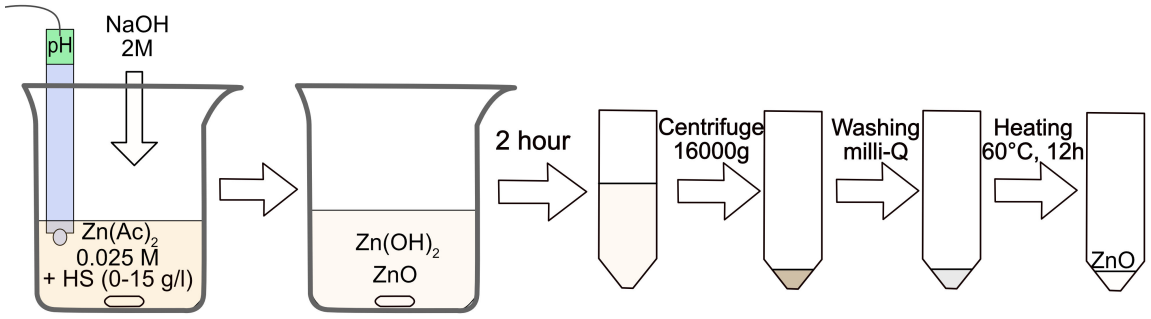

FIG. 1. Scheme of synthesis of Humic-ZnO nanocomposites in media containing humic substances

We prepared a solution of sodium humate in Milli-Q water at concentrations of 0.1, 0.5, 1, 2, 4, 8, and 15 g/L. Then, a volume of 50 ml of the prepared CHP solution was placed into a glass equipped with a dropping funnel filled with 2M NaOH and an electrode was inserted for pH measurements during synthesis. A volume of 50 mL of 0.025M zinc acetate was prepared and added dropwise to the CHP solution under continued stirring and pH adjustment to 12 by adding 2M NaOH. The resulting solution was stirred with a magnetic stirrer for 2 hours at room temperature. Then, the settled down sediment was separated and washed by multiple centrifugations at 16000 g with Milli-Q water to remove salts and unbound humic material. The precipitate was dried in a vacuum oven at 60°C for 12 hours. The obtained precipitates were from light grey to light brown in color. They were designated as ZnO–PX, where X is the concentration of CHP during synthesis (g/L).

2.3. Characterisation of humic zinc oxide nanocomposites

The obtained products were characterized using powder X-ray diffraction (PXRD) analysis to determine phase composition and crystallite size of the synthesized ZnO-HS-nanocomposites. We used a D/MAX 2500 (Rigaku, Japan) rotating anode diffractometer (Rigaku, Tokyo, Japan) in reflection geometry (Bragg-Brentano) with Cu $Ka_{1,2}$ radiation and a graphite monochromator. The PXRD patterns were collected in a range from 5 to 80°2θ with a step of 0.02. Phase analysis was performed using Match 3 software, whereas corresponding to zinc oxide nanoparticles size coherent scattering region (CSR) was evaluated with anisotropic model using MAUD software [41].

Size and morphology of the ZnO-HS nanocomposites were investigated using a high-resolution transmission electron microscope (TEM) JEM-2100 F (JEOL, Japan) at an accelerating voltage of 200 kV. Prior to analysis, the dry ZnO-NPs samples were ultrasonically dispersed in Milli-Q water, and a drop of sample was applied to carbon coated copper grid and dried.

UV-vis spectroscopy Cary 50 (Varian, USA) was used to measure the absorbance of ZnO–NPs to determine the band gap width and exciton energy. For the measurements, powder samples of all ZnO–NPs were ultrasonically treated in Milli-Q water.

Conversion degree of ionic Zn was determined by measuring Zn concentration in the supernatants after separation of sediments using inductively coupled plasma atomic emission spectrometry (ICP–AES) on an Agilent 5100 instrument. The concentration of Zn in the supernatants ranged from 0.1 to 0.5 mM, which corresponds to a conversion degree of 98–99% of ionic Zn to ZnO under the conditions used in the described above experimental setup.

2.4. Preparation of gels filled with ZnO-HS nanocomposites

For gel preparation, a weight of ZnO-NP-HS was ultrasonically dispersed in Milli-Q water to yield a concentration of 2% on metallic zinc basis. Then a weight of CMC (2% by mass) was added to the solution with dispersed nanocomposites and vigorously mixed with a glass rod to obtain homogeneous solution. Intense gelation started within first 10 minutes, and continued until complete homogenization was achieved in 30 minutes under continued mechanical agitation.

2.5. Setup of zinc release experiments from gels

A nitrocellulose membrane (0.5, 3, 13.5 kDa, Merck, Germany) was used to study zinc release. The membrane was attached to one end of a plastic tube, 1.5 cm in diameter and 2 cm long. An amount of gel having a weight of 2 g was placed in a tube. The tube filled with gel was placed atop of a 50 mL tube filled with a buffer solution, so that only the membrane surface touched the solution. We used Mueller-Hinton broth (Dehydrated infusion from beef 0.3 g/L, Casein hydrolysate 0.0175 g/L, Starch 0.0015 g/L, Agar, pH 7.3), 0.1M acetate buffer (pH 5.5) and Milli-Q water for release experiments. To imitate conditions of human body, the test compositions were kept in a thermostat at 37°C. The samples were collected after 2, 4, 6, 8, 24, 48, 56.5, 79, 145.5, 247 hours. The aliquot was diluted with 5% nitric acid and analyzed after a thorough mixing and settled for 1 h using an Agilent 5100 inductively coupled plasma spectrometer (ICP-AES). The scheme and photo of the experiment installation are shown in Fig. 2. All experiments were carried out in three replicates. To account for measurement error mean percent standard deviation was evaluated.

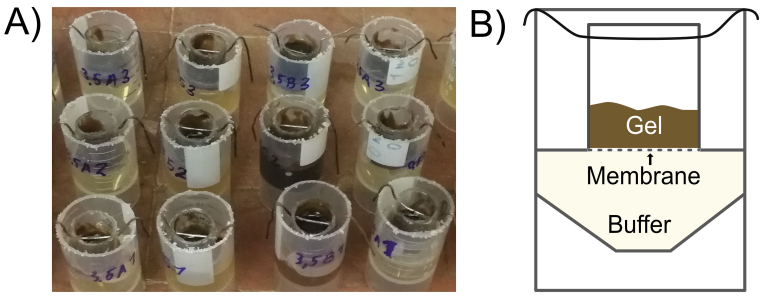

FIG. 2. Photo (A) and scheme (B) of equipment for the investigation of zinc release

3. Results and discussion

3.1. Characterisation of ZnO-NP-HS nanocomposites

ZnO-HS nanocomposites were synthesized using concentrations of HS in the range from 0.1 to 15 g/L. The PXRD results (Fig. 3A) confirmed the presence of characteristic peaks of ZnO in the samples obtained. At the same time, at high concentrations of HS – 4, 8, and 15 g/L, characteristic peaks of $Zn(OH)_2$ of low intensity were also detected, which may be associated with its binding and stabilization with HS.

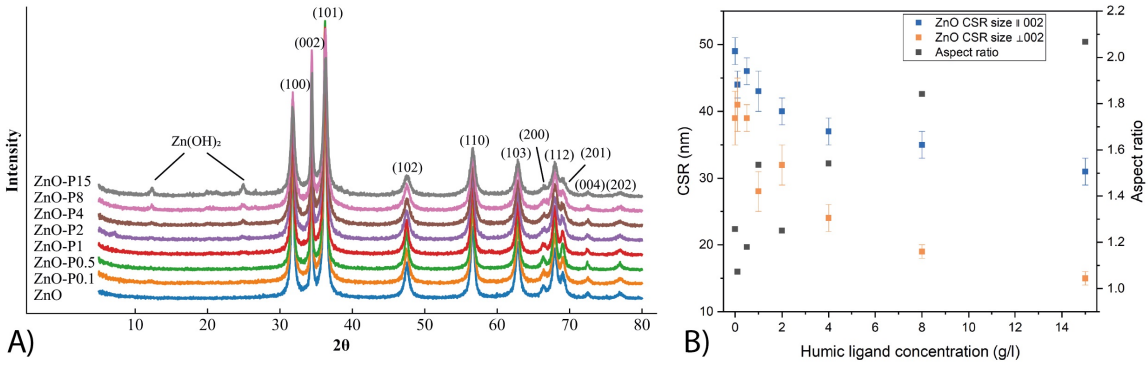

FIG. 3. PXRD patterns of ZnO-HS nanocomposites synthesised in the presence of increasing concentrations of HS (0, 0.1, 2, 4, 8, 15 g/L) (A), HS concentration effect on the calculated CSR sizes and aspect ratio of ZnO nanoparticles (B)

The NP sizes calculated from the PXRD data (Fig. 3B) ranged from 15 to 45 nm decreasing gradually with an increase in concentration of the humic ligand. In this case, the sizes of ZnO nanoparticles monotonously decrease both along the 002 direction and in the perpendicular direction, whereas aspect ratio rises. The observed phenomenon could be caused by an inhibition of $Zn(OH)_2$ crystallite growth due to blocking growth facets via binding with humic ligands similar to mechanism for feroxyhyte NPs which was described by [42]. However, when measured with TEM (Fig. 4), the synthesized composites turned out to be composed of the NPs aggregated into much larger – micron size, star-shaped particles. It can be explained by the peculiarity of ZnO particle size determination with X-ray diffraction, where the size of the coherent scattering region is calculated. In contrast, TEM measures size of the whole aggregate.

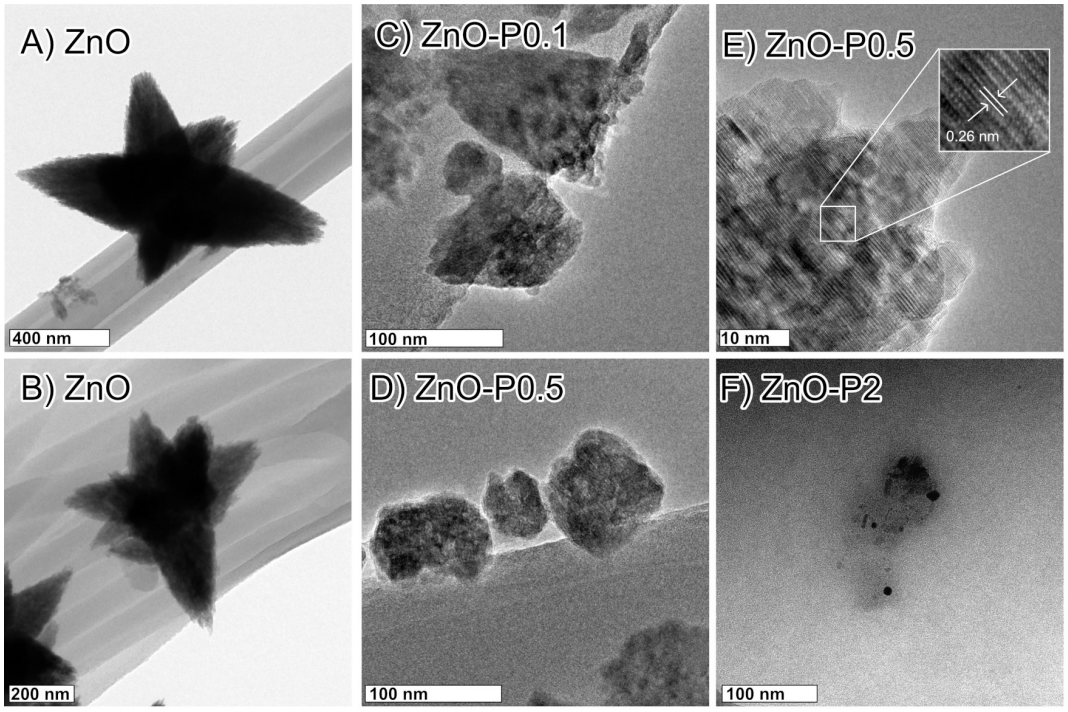

FIG. 4. TEM images of ZnO synthesized in the absence of HS (A, B), in the presence of 0.1 g/L HS (C), 0.5 g/L HS (D, E) and 2 g/L HS (F)

The TEM images show that the sizes of the obtained particles are in the micrometer range. The largest particles (near 1 μm) are observed for the preparations obtained without humic ligands. In the presence of humic ligands, particles are formed with sizes of 50–200 nm. Humic ligands change not only size, but morphology of particles as well. In the absence of humic ligands (Fig. 4A,B), star-shaped aggregates are formed, which consist of single ZnO particles of 400–800 nm in size (Fig. 4B). In the presence of HS (Fig. 4C-F), both large aggregates and small particles are visible. As HS concentration increases, the particle size decreases down to 50–100 nm (0.1 g/L), 30–100 nm (0.5 g/L), and 10–30 nm (2 g/L), which is consistent with the PXRD data. When examining the large-scale images (Fig. 3E), the crystal structure with an interplanar distance of 0.26 nm perpendicular to the plane 002 of ZnO can be seen.

To evaluate the band gap width of zinc oxide nanoparticles obtained with humic substance addition optical absorption spectra were collected. Absorption coefficients (α) were calculated from measured spectra using Kubelka-Munk theory:

$$F(R) = \frac{(1-R)^2}{2R^2} = \frac{\alpha}{s},$$

where $F(R)$ is the Kubelka-Munk function, R is the reflectance, s is the scattering coefficient.

The obtained spectra were transformed into the Tauc plot for allowed direct electron transition (Fig. 5A):

$$\alpha h\nu \sim (h\nu - E_g)^{1/2},$$

where E_g is the band gap.

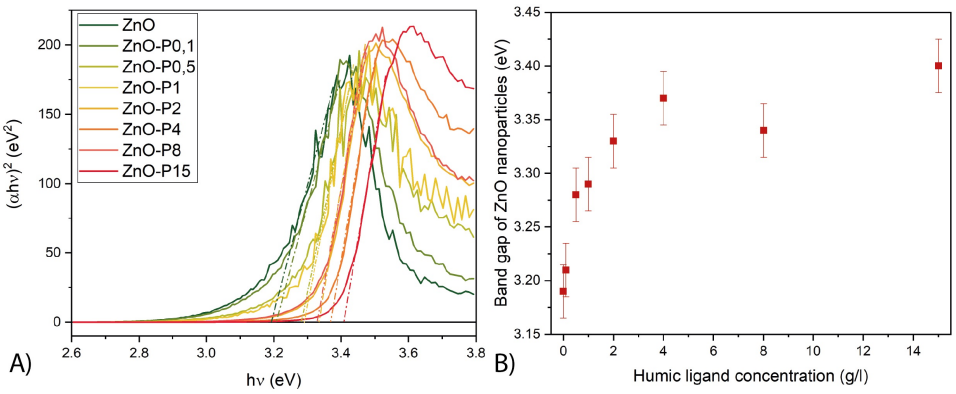

FIG. 5. Tauc plot of the humic zinc oxide nanocomposites UV-vis absorbance spectra (A). The HS concentration effect on the ZnO nanoparticles band gap (B)

The UV-vis absorption curves have a typical for ZnO characteristic absorption edge and exciton peak at 3.2–3.6 eV range. With increasing concentration of the humic ligand during synthesis, the observed absorption edge shifts to the larger energies. Also calculated zinc oxide nanoparticles band gap monotonously rises, that possibly is caused by the decrease in the size of individual crystallites of zinc oxide crystallites (Fig. 5B).

The calculated band gap values for ZnO nanoparticles and their size-dependent behavior are in good agreement with the reported data [43, 44]. It can be explained by decreasing the ZnO nanoparticles sizes caused by addition with HS during synthesis. Thus, the presence of HS allows us to control the ZnO nanoparticles sizes and to tune their band gap width, increasing it up to 3.40 eV at HS concentration of 15 g/L.

As can be seen from the above data, the use of humic substances leads to a significant change in the morphology of zinc oxide nanoparticles. The presence of humic substance both stabilizes the smaller ZnO crystallites and prevents its further aggregation. It also should be emphasised that a relatively high concentration of humic substances, from 4 g/L, is needed to observe a significant effect. This concentration is much higher than the typical maximum for natural content in water (up to 0.2 g/L), and the effect of this concentration range on ZnO nanoparticles was investigated earlier [20]. However, for the directed synthesis of drugs, the use of these concentrations is quite justified, since humic substances retain their neutral properties even at high concentrations.

3.2. Filling gels with ZnO-HS nanocomposites and zinc slow release

When the humic ZnO nanocomposites are dispersed, a non-viscous suspension is obtained, which is inconvenient to apply in the case of wounds. For wound treatment, gels and ointments are widely used, the advantage of which is high viscosity and more prolonged exposure of active substances to the wound. Therefore, in this work, we used commercially available preparations of carboxymethylcellulose (CMC) as gel carriers, which are widely used to create gels that are convenient and safe, including for the creation of medical preparations for external use. For gel preparation, ZnO samples were dispersed in water at a concentration of 2% zinc and then the gel matrix was added and stirred vigorously for 30 minutes until the gel swelled to a halt. Fig. 6 shows photo (A, B) of gel making filled with ZnO-P15 nanocomposites and SEM image (C, D).

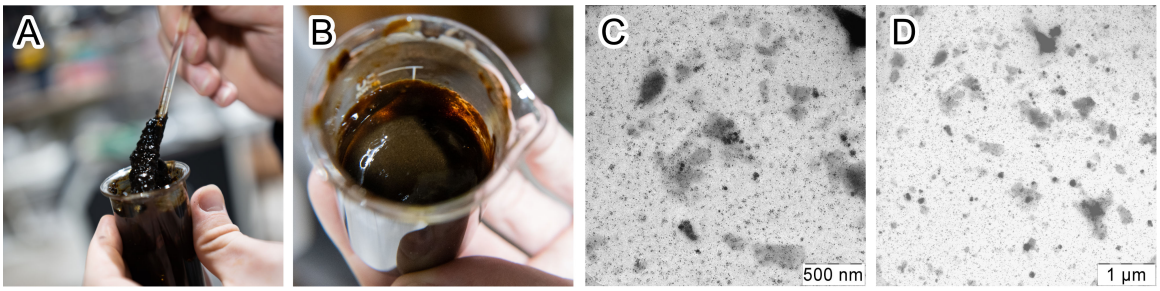

FIG. 6. Photo of Gel preparations filled with ZnO-P15 nanocomposites (A, B) and SEM image of them (C, D)

The resulting gels are quite dense, do not spread on the surface, and are able to hold the liquid containing active ingredients in its composition. The TEM results (Fig. 6 C,D) for this gel show the presence of a wide distribution of particle size in it, from small, 10–20 nm, to large 200–500 nm aggregates.

For wound healing dressing, the active ingredients must be slowly released. In this case, as a result of the influence of the wound environment and various anions, zinc nanoparticles are gradually destroyed with the release of zinc, which has an antibacterial and wound-healing effect. The anions diffuse into the gel and dissolve the zinc oxide, resulting in the release of zinc as a Zn^{2+} ions. To study kinetics of this process, the release of zinc in Mueller-Hinton broth and 0.1M acetate buffer (pH 5.5) was studied through membranes with different pore diameters: large (13.5 kDa) intermediary (3.5 kDa) and small (0.5 kDa), and the data obtained are shown in Fig. 7.

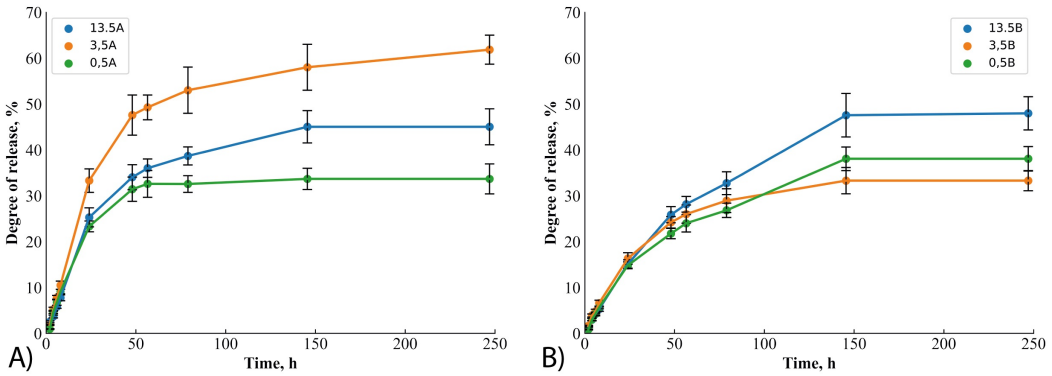

FIG. 7. Kinetics of the zinc release from CMC gel, A - acetate buffer, B - Mueller-Hinton broth, pore diameter of the dialysis membrane: 13.5 (highlighted in blue), 3.5 (highlighted in orange) and 0.5 kDa (highlighted in green), respectively

It can be seen that zinc is released into the acetate buffer at the higher rate (Fig. 7A) as compared to the Mueller-Hinton broth (Fig. 7B), which is manifested as the steeper slope of the release plots in Fig. 7B. At the same time, the total amount of zinc released is larger for the Mueller-Hinton broth as compared to the acetate buffer. Against the expectations, the largest zinc release was observed for the membrane with intermediary pore size (3.5 kDa) in case of the acetate buffer, where it achieved (50±10) %. At the same time, this very membrane was characterized with the minimum zinc release into the Muller Hinton broth of (30 ±5%). Such a discrepancy in the expected and factual values of zinc release through this membrane might be indicative of its biased behavior for the systems used in this study.

The zinc release from the gel reached its equilibrium after 150 hours of exposure on all three permeable membranes used in this study. The amount of zinc transferred into the solution over this exposure time accounted for (40 ± 10) % of its total content in the gel both for the large and small membranes. For the intermediary membrane, the released amount varied substantially for Mueller-Hinton broth versus acetate buffer and accounted for 30 and 60%, respectively. Of importance is that a substantial portion of zinc (from 10 to 15% of its total content in the gel) zinc was released during the first 24 hours, which gives good promise for the long-term effect of the carboxymethylcellulose gels filled with ZnO-HS nanocomposites.

4. Conclusions

In this work, we showed that the humic substances can be used effectively in the wet precipitation synthesis of zinc oxide nanoparticles within concentrations up to 15 g/L facilitating the formation and stabilization of zinc oxide nanoparticles. HS inhibits the growth of ZnO nanoparticles by blocking growth facets similar to mechanism described in the

literature for feroxyhyte NPs [41]. This phenomenon brings about formation of smaller nanoparticles. These nanosize-effects of HS with respect to ZnO particles were experimentally evidenced with a use of PXRD and UV-vis spectroscopy measurements. The nanocomposites obtained can be efficiently used for the treatment of wounds due to beneficial combination of properties of the both components: ZnO-NPs might act as antibacterial agents, whereas HS could prevent cytotoxicity and rapid consumption of Zn-NPs. The most preferable treatment form for wound healing applications are hydrogels. This is why we filled in 2% solution of carboxymethylcellulose with the ZnO–HS nanocomposites and studied zinc release from the filled gels. The results showed that zinc is released slowly, about 10–30% of the total amount for the first day. This allowed us to conclude that the CMC gels filled with ZnO-HS nanocomposites could be used as a slow-release zinc applications in wound healing.

References

[1] Nandhini S.N., Sisubalan N., Vijayan A., Karthikeyan C., Gnanaraj M., Gideon D.A.M., Jebastin T., Varaprasad K., Sadiku R. Recent advances in green synthesized nanoparticles for bactericidal and wound healing applications. *Heliyon*, 2023, **9**, P. e13128.

[2] Pino P., Bosco F., Mollea C., Onida B. Antimicrobial Nano-Zinc Oxide Biocomposites for Wound Healing Applications: A Review. *Pharmaceutics*, 2023, **15**, P. 970.

[3] Singh M., Thakur V., Kumar V., Raj M., Gupta S., Devi N., Upadhyay S.K., Macho M., Banerjee A., Ewe D., Saurav K. Silver Nanoparticles and Its Mechanistic Insight for Chronic Wound Healing: Review on Recent Progress. *Molecules*, 2022, **27**, P. 5587.

[4] Mishra P.K., Mishra H., Ekielski A., Talegaonkar S., Vaidya B. Zinc oxide nanoparticles: a promising nanomaterial for biomedical applications. *Drug Discovery Today*, 2017, **22**, P. 1825–1834.

[5] Vasile B.S., Oprea O., Voicu G., Ficai A., Andronescu E., Teodorescu A., Holban A. Synthesis and characterization of a novel controlled release zinc oxide/gentamicin–chitosan composite with potential applications in wounds care. *International journal of pharmaceutics*, 2014, **463**, P. 161–169.

[6] Mohandas A., PT S.K., Raja B., Lakshmanan V.K., Jayakumar R. Exploration of alginate hydrogel/nano zinc oxide composite bandages for infected wounds. *International journal of nanomedicine*, 2015, **10**, P. 53–66.

[7] Sirelkhatim A., Mahmud S., Seeni A., Kaus N.H.M., Ann L.C., Bakhori S.K.M., Hasan H., Mohamad D. Review on Zinc Oxide Nanoparticles: Antibacterial Activity and Toxicity Mechanism. *Nano-Micro Lett*, 2015, **7**, P. 219–242.

[8] Shaba E.Y., Jacob J.O., Tijani J.O., Suleiman M.A.T. A critical review of synthesis parameters affecting the properties of zinc oxide nanoparticle and its application in wastewater treatment. *Appl Water Sci*, 2021, **11**, P. 48.

[9] Zheng J.H., Jiang Q., Lian J.S. Synthesis and optical properties of flower-like ZnO nanorods by thermal evaporation method. *Applied Surface Science*, 2011, **257**, P. 5083–5087.

[10] Gerbreders V., Krasovska M., Sledevskis E., Gerbreders A., Mihailova I., Tamanis E., Ogurcovs A. Hydrothermal synthesis of ZnO nanostructures with controllable morphology change. *CrystEngComm*, 2020, **22**, P. 1346–1358.

[11] Hasnidawani J.N., Azlina H.N., Norita H., Bonnia N.N., Ratim S., Ali E.S. Synthesis of ZnO Nanostructures Using Sol-Gel Method. *Procedia Chemistry*, 2016, **19**, P. 211–216.

[12] Wojnarowicz J., Chudoba T., Lojkowski W. A Review of Microwave Synthesis of Zinc Oxide Nanomaterials: Reactants, Process Parameters and Morphologies. *Nanomaterials*, 2020, **10**, P. 1086.

[13] Zhang F. Grand Challenges for Nanoscience and Nanotechnology in Energy and Health. *Front. Chem.*, 2017, **5**, P. 80.

[14] Arati Sharma S.V.M., Robertson G.P. Toxicological considerations when creating nanoparticle-based drugs and drug delivery systems. *Expert Opinion on Drug Metabolism & Toxicology*, 2012, **8**, P. 47–69.

[15] Hühn D., Kantner K., Geidel C., Brandholt S., De Cock I., Soenen S.J.H., Rivera Gil P., Montenegro J.-M., Braeckmans K., Müllen K., Nienhaus G.U., Klapper M., Parak W.J. Polymer-Coated Nanoparticles Interacting with Proteins and Cells: Focusing on the Sign of the Net Charge. *ACS Nano*, 2013, **7**, P. 3253–3263.

[16] Sathiyaseelan A., Vishven Naveen K., Zhang X., Han K., Wang M.-H. Research progress on chitosan-zinc oxide nanocomposites fabrication, characterization, biomedical and environmental applications. *Coordination Chemistry Reviews*, 2023, **496**, P. 215398.

[17] Agban Y., Mugisho O.O., Thakur S.S., Rupenthal I.D. Characterization of Zinc Oxide Nanoparticle Cross-Linked Collagen Hydrogels. *Gels*, 2020, **6**, P. 37.

[18] Shahvalizadeh R., Ahmadi R., Davandeh I., Pezeshki A., Seyed Moslemi S.A., Karimi S., Rahimi M., Hamishehkar H., Mohammadi M. Antimicrobial bio-nanocomposite films based on gelatin, tragacanth, and zinc oxide nanoparticles – Microstructural, mechanical, thermo-physical, and barrier properties. *Food Chemistry*, 2021, **354**, P. 129492.

[19] Parani M., Lokhande G., Singh A., Gaharwar A.K. Engineered Nanomaterials for Infection Control and Healing Acute and Chronic Wounds. A*CS Appl. Mater. Interfaces*, 2016, **8**, P. 10049–10069.

[20] Šebesta M., Kolenčík M., Urík M., Bujdoš M., Vávra I., Dobročcka E., Smilek J., Kalina M., Diviš P., Pavúk M., Miglierini M., Kratošová G., Matúš P. Increased Colloidal Stability and Decreased Solubility—Sol—Gel Synthesis of Zinc Oxide Nanoparticles with Humic Acids. *J. Nanosci. Nanotechnol*, 2019, **19**, P. 3024–3030.

[21] Hayes M., MacCarthy P., Malcolm R., Swift R. The search for structure: setting the scene. Humic substances II, in search of struture. *Chichester, John, Wiley & Sons*, 1989, P. 3–33.

[22] Nebbioso A., Piccolo A. Basis of a Humeomics Science: Chemical Fractionation and Molecular Characterization of Humic Biosuprastructures. *Biomacromolecules*, 2011, **12**, P. 1187–1199.

[23] Ji Y., Zhang A., Chen X., Che X., Zhou K., Wang Z. Sodium humate accelerates cutaneous wound healing by activating TGF-β/Smads signaling pathway in rats. *Acta Pharmaceutica Sinica B*, 2016, **6**, P. 132–140.

[24] Lipczynska-Kochany E., Kochany J. Humic substances in bioremediation of industrial wastewater—Mitigation of inhibition of activated sludge caused by phenol and formaldehyde. *Journal of Environmental Science and Health, Part A*, 2008, **43**, P. 619–626.

[25] Wan J., Dong W., Tokunaga T.K. Method to Attenuate U(VI) Mobility in Acidic Waste Plumes Using Humic Acids. *Environ. Sci. Technol.*, 2011, **45**, P. 2331–2337.

[26] Liu J.F., Zhao Z.S., Jiang G.B. Coating Fe_3O_4 magnetic nanoparticles with humic acid for high efficient removal of heavy metals in water. *Environmental science & technology*, 2008, **42**, P. 6949–6954.

[27] Polyakov A.Yu., Lebedev V.A., Shirshin E.A., Rumyantsev A.M., Volikov A.B., Garshev A.V., Goodilin E.A., Perminova I.V. Non-classical growth of water-redispersible spheroidal gold nanoparticles assisted by leonardite humate. *Cryst. Eng. Comm.*, 2017, **19**, P. 876–886.

[28] Ghosh S., Jiang W., McClements J.D., Xing B. Colloidal stability of magnetic iron oxide nanoparticles: Influence of natural organic matter and synthetic polyelectrolytes. *Langmuir*, 2011, **27**, P. 8036–8043.
[29] Kulikova N.A., Polyakov A.Y., Lebedev V.A., Abroskin D.P., Volkov D.S., Pankratov D.A., Klein O.I., Senik S.V., Sorkina T.A., Garshev A.V., Veligzhanin A.A., Garcia Mina J.M., and Perminova I.V. Key roles of size and crystallinity of nanosized iron (hydr)oxides stabilized by humic substances in iron bioavailability to plants. *Journal of Agricultural and Food Chemistry*, 2017, **65**(51), P. 11157–11169.
[30] Sorkina T.A., Polyakov A.Yu., Kulikova N.A., Goldt A.E., Philippova O.I., Aseeva A.A., Veligzhanin A.A., Zubavichus Ya.V., Pankratov D.A., Goodilin E.A., Perminova I.V. Nature-inspired soluble iron-rich humic compounds: new look at the structure and properties. *Journal of Soils and Sediments*, 2014, **14**(2), P. 261–268.
[31] Perminova I.V. Humic substances-assisted synthesis of nanoparticles in the nature and in the lab. In Functions of Natural Organic Matter in Changing Environment. Eds. J. Xu, J. Wu, Y. He. Zhejiang University Press and Springer Science+Business Media, Dordrecht, 2013 P. 735–740.
[32] Schepetkin I.A., Khlebnikov A.I., Ah S.Y., Woo S.B., Jeong C.-S., Klubachuk O.N., Kwon B.S. Characterization and biological activities of humic substances from mumie. *J. Agric. Food Chem.*, 2003, **51**, P. 5245–5254.
[33] Jayakumar R., Sudheesh Kumar P., Mohandas A., Lakshmanan V.-K., Biswas R. Exploration of alginate hydrogel/nano zinc oxide composite bandages for infected wounds. *IJN*, 2015, **53**.
[34] Sherafatkhah Azari S., Alizadeh A., Roufegarinejad L., Asefi N., Hamishehkar H. Preparation and characterization of gelatin/β-glucan nanocomposite film incorporated with ZnO nanoparticles as an active food packaging system. *J. Polym. Environ*, 2021, **29**, P. 1143–1152.
[35] Nafchi A.M., Alias A.K., Mahmud S., Robal M. Antimicrobial, rheological, and physicochemical properties of sago starch films filled with nanorod-rich zinc oxide. *Journal of Food Engineering*, 2012 **113**, P. 511–519.
[36] Ismail S.H., Hamdy A., Ismail T.A., Mahboub H.H., Mahmoud W.H., Daoush W.M. Synthesis and characterization of antibacterial Carbopol/ZnO hybrid nanoparticles gel. *Crystals*, 2021, **11**, 1092.
[37] Sakohara S., Mori K. Preparation of ZnO nanoparticles in amphiphilic gel network. *J Nanopart Res*, 2008, **10**, P. 297–305.
[38] Rakhshaei R., Namazi H. A potential bioactive wound dressing based on carboxymethyl cellulose/ZnO impregnated MCM-41 nanocomposite hydrogel. *Materials Science and Engineering: C*, 2017, **73**, P. 456–464.
[39] Yadollahi M., Gholamali I., Namazi H., Aghazadeh M. Synthesis and characterization of antibacterial carboxymthyl cellulose/ZnO nanocomposite hydrogels. *International Journal of Biological Macromolecules*, 2015, **74**, P. 136–141.
[40] Zafar A., Khosa M.K., Noor A., Qayyum S., Saif M.J. Carboxymethyl Cellulose/Gelatin Hydrogel films loaded with Zinc Oxide nanoparticles for sustainable food packaging applications. *Polymers*, 2022, **14**, P. 5201.
[41] Lutterotti L. Total pattern fitting for the combined size–strain–stress–texture determination in thin film diffraction. *Nuclear Instruments and Methods in Physics Research Section B: Beam Interactions with Materials and Atoms*, 2010, **268**(3-4), P. 334–340.
[42] Polyakov A.Yu, Goldt A.E., Sorkina T.A., Perminova I.V., Pankratov D.A., Goodilin E.A., Tretyakov Y.D. Constrained growth of anisotropic magnetic δ-FeOOH nanoparticles in the presence of humic substances *CrystEngComm*, 2012, **14**(23), P. 8097–8102.
[43] Goh E.G., Xu X., McCormick P.G. Effect of particle size on the UV absorbance of zinc oxide nanoparticles. *Scripta Materialia*, 2014, **78–79**, P. 49–52.
[44] Arif A., Belahssen O., Gareh S., Benramache S. The calculation of band gap energy in zinc oxide films. *J. Semicond*, 2015, **36**, P. 013001.

Submitted 9 November 2023; revised 19 November 2023; accepted 20 November 2023

Information about the authors:

Konstantin S. Larionov – Department of Chemistry, Lomonosov Moscow State University, Leninskiye Gory 1-3, 119991 Moscow, Russia; ORCID 0009-0009-1635-3648; konstantin.larionov@chemistry.msu.ru

Alexander Volikov – Department of Chemistry, Lomonosov Moscow State University, Leninskiye Gory 1-3, 119991 Moscow, Russia; ORCID 0000-0002-8475-8091; ab.volikov@gmail.com

Nikita A. Sobolev – Department of Chemistry, Lomonosov Moscow State University, Leninskiye Gory 1-3, 119991 Moscow, Russia; ORCID 0000-0002-8210-8263; n.a.sobolev@outlook.com

Daniil A. Kozlov – Kurnakov Institute of General and Inorganic Chemistry of RAS, Leninsky Prospect 31, 119991 Moscow, Russia; ORCID 0000-0003-0620-8016; kozlov@inorg.chem.msu.ru

Irina V. Perminova – Department of Chemistry, Lomonosov Moscow State University, Leninskiye Gory 1-3, 119991 Moscow, Russia; ORCID 0000-0001-9084-7851; iperm@med.chem.msu.ru

Conflict of interest: the authors declare no conflict of interest.